ACS chemical biology

Letters

pubs.acs.org/acschemicalbiology

In Vitro Demonstration of Apoptosis Mediated Photodynamic Activity and NIR Nucleus Imaging through a Novel Porphyrin

Suneesh C. Karunakaran,[†] P. S. Saneesh Babu,[‡] Bollapalli Madhuri,[§] Betsy Marydasan,[†] Albish K. Paul,[†] Asha S. Nair,[‡] K. Sridhar Rao,[§] Alagar Srinivasan,[∥] Tavarekere K. Chandrashekar,*[,∥] Ch. Mohan Rao,*[,§] Radhakrishna Pillai,*[,‡] and Danaboyina Ramaiah*[,†]

[†]Chemical Sciences and Technology Division, Photosciences and Photonics, CSIR-National Institute for Interdisciplinary Science and Technology (CSIR-NIIST), Trivandrum-695019, Kerala, India

[‡]Rajiv Gandhi Centre for Biotechnology, Trivandrum-695014, Kerala, India

[§]CSIR-Centre for Cellular and Molecular Biology (CSIR-CCMB), Hyderabad-500 007, Andhra Pradesh, India

[∥]National Institute of Science Education and Research (NISER), Bhubaneswar-751005, Odisha, India

Supporting Information

ABSTRACT: We synthesized a novel water-soluble porphyrin **THPP** and its metalated derivative **Zn-THPP** having excellent triplet excited state quantum yields and singlet oxygen generation efficiency. When compared to U.S. Food and Drug Administration approved and clinically used sensitizer Photofrin, **THPP** showed *ca.* 2−3-fold higher *in vitro* photodynamic activity in different cell lines under identical conditions. The mechanism of the biological activity of these porphyrin systems has been evaluated through a variety of techniques: 3-(4,5-dimethylthiazol-2-yl)-2,5-diphenyltetrazolium bromide (MTT) assay, comet assay, poly(ADP-ribose)-polymerase (PARP) cleavage, CM-H_2DCFDA assay, DNA fragmentation, flow cytometric analysis, fluorescence, and confocal microscopy, which confirm the apoptotic cell death through predominantly reactive oxygen species (ROS). Moreover, **THPP** showed rapid cellular uptake and are localized in the nucleus of the cells as compared to Hoechst dye and Photofrin, thereby demonstrating its use as an efficient sensitizer in photodynamic therapy and live cell NIR nucleus imaging applications.

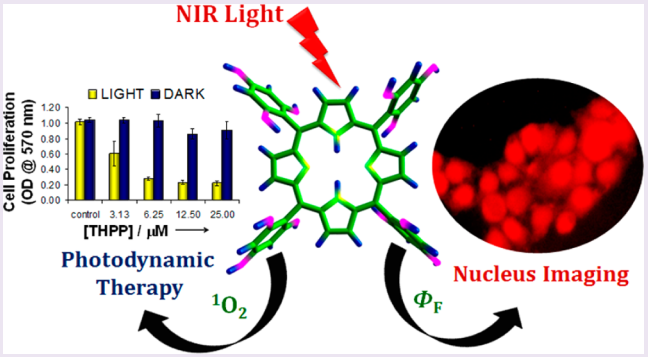

Photodynamic therapy (PDT) is an emerging treatment for different types of cancers.[1−4] It involves the inactivation of living cells by the combined action of light, a photoactive molecule called sensitizer and molecular oxygen.[5−7] A variety of sensitizers have been examined for their use in PDT. These include porphyrins, chlorins, bacteriochlorins, phthalocyanines, metallophthalocyanines, porphycenes, squaraines, cyanines, rose bengal, methylene blue, aminolevulinic acid, and their derivatives.[8−11] Among these, porphyrins have attracted much attention as sensitizers due to their higher cellular affinity and very low dark toxicity.[12−14] For example, the hematoporphyrin derivative (HpD) and its commercial variant, i.e., Photofrin, is being currently used in the treatment of various types of cancers.[15−17] However, HpD is a mixture of at least nine components, causes cutaneous photosensitivity and immunosuppression, and, more importantly, has only a weak absorption in the red region of the spectrum.[18,19] The drawbacks associated with the first generation photosensitizer HpD have provided the great impetus to search for new photosensitizers with greater specificity and efficacy.[20,21] In this context, we designed a novel porphyrin derivative **THPP** and have investigated its photophysical and *in vitro* photobiological properties when compared to its zinc complex, **Zn-THPP**, and U.S. Food and Drug Administration approved and clinically used sensitizer, Photofrin. Interestingly, **THPP** showed high solubility in buffer and significant quantum yields of triplet excited state and singlet oxygen generation. Uniquely, **THPP** exhibited *ca.* 2−3-fold high photocytotoxicity and localized specifically in the nucleus when compared to Photofrin, indicating thereby its potential as an efficient sensitizer for PDT and NIR imaging applications.

Synthesis of the new porphyrin derivatives **THPP** and **Zn-THPP** was achieved through the modified Lindsey's method[22,23] (Scheme 1) and were characterized on the basis of elemental analysis and spectral evidence (Supplementary Figures 1 and 2). These derivatives showed high solubility in alcoholic solvents and aqueous medium. The free base **THPP** showed the characteristic absorption of the porphyrin chromophore having a Soret band at 416 nm and four Q-bands at 514, 548, 592, and 648 nm, while its fluorescence

Received: August 31, 2012
Accepted: October 23, 2012
Published: October 23, 2012

   dx.doi.org/10.1021/cb3004622 | *ACS Chem. Biol.* 2013, 8, 127−132

Scheme 1. Synthesis of Porphyrins THPP and Zn-THPP

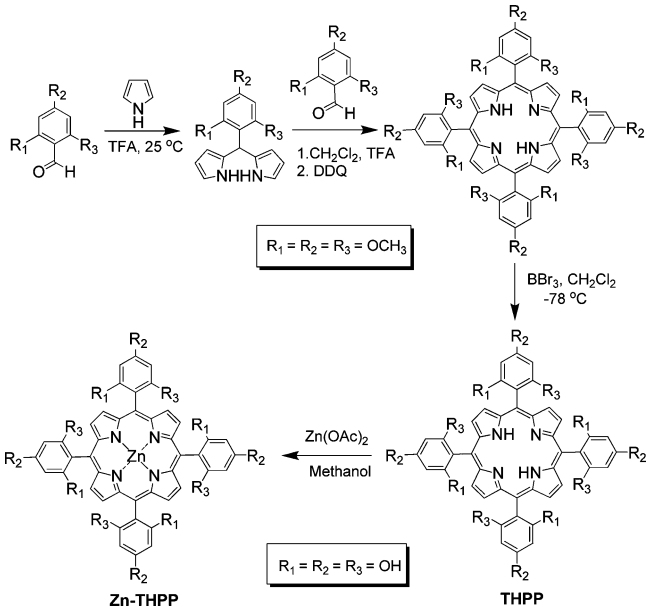

spectrum exhibited two emission maxima at 645 and 709 nm (Figure 1a,b). The complex, **Zn-THPP**, similarly exhibited a bathochromically shifted (*ca.* 7 nm) Soret absorption at 423 nm and two Q-bands at 555 and 595 nm, whereas two emission bands were centered at 606 and 656 nm (Supplementary Figure 3). The emission quantum yields (Φ_F) were calculated and are found to be 0.08 ± 0.002 and 0.03 ± 0.001, for **THPP** and **Zn-THPP**, respectively, in water.

To understand the transient intermediates involved in these systems, we have carried out nanosecond laser flash photolysis studies employing a 532 nm laser pulse (Figure 1c). The transient absorption spectrum of **THPP** obtained after the laser excitation in methanol showed an absorption maximum at 460 nm with a bleach at 420 nm, where the compound has significant ground state absorption. The lifetime of the transient was calculated from the decay profile at 460 nm (Inset of Figure 1c) and is found to be 12 μs. The transient formed was characterized as a triplet excited state of **THPP** based on the quenching experiments and its negligible formation in the presence of dissolved oxygen. Similar observations were made with **Zn-THPP**. This complex showed the triplet excited state absorption maximum at 450 nm and lifetime of 20 μs in methanol (Supplementary Figure 4). The quantum yields of triplet excited states (Φ_T) were estimated using triplet−triplet energy transfer method to β-carotene and $[Ru(bpy)_3]^{2+}$ as the standard.[24,25] The values in methanol are Φ_T = 0.66 ± 0.05 and 0.94 ± 0.02, for **THPP** and **Zn-THPP**, respectively.

In addition to favorable photophysical properties, the PDT efficacy of a sensitizer depends on its efficiency of singlet oxygen generation. Therefore, we have determined quantum yields [$\Phi(^1O_2)$] of singlet oxygen by using 1,3-diphenylisobenzofuran (DPBF) as the singlet oxygen scavenger. To calculate the yields, the sensitizer along with DPBF was irradiated using a xenon lamp with a 515 nm LP filter at different time intervals from 0 to 30 s. The decrease in the absorbance of DPBF was monitored at 410 nm and compared with those observed with the standard, tetra(*meta*-hydroxyphenyl)porphyrin (*m*-**THPP**) under identical conditions.[26,27] From the slope of the graph obtained by plotting the change in absorbance of DPBF against the time of irradiation (Figure 1d), we calculated singlet oxygen quantum yields. These values are $\Phi(^1O_2)$ = 0.59 ± 0.03 for **THPP** and 0.92 ± 0.02 for **Zn-THPP** in methanol.

To investigate *in vitro* photodynamic activity (PDT) of these derivatives, we employed MTT assay in three different cancer

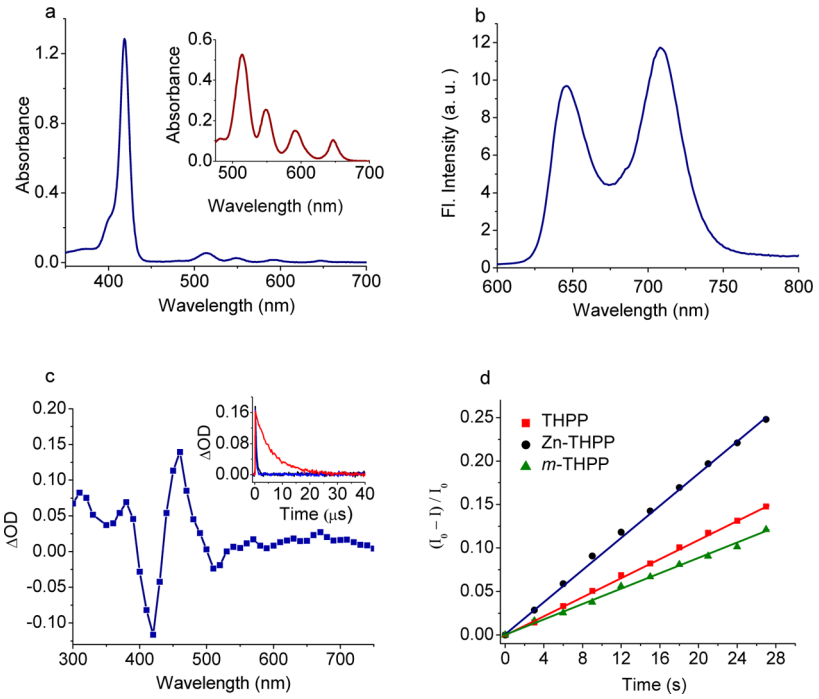

Figure 1. (a) UV−vis absorption and (b) fluorescence (λ_{ex}, 430 nm) spectra of **THPP** (4 μM) in water. (c) Triplet transient absorption spectrum with decay at 460 nm (inset) of **THPP** (20 μM) in methanol and (d) plot of changes in absorption of 1,3-diphenylisobenzofuran with **THPP**, **Zn-THPP**, and *m*-**THPP** (515 nm LP) versus irradiation time in methanol.

dx.doi.org/10.1021/cb3004622 | *ACS Chem. Biol.* 2013, 8, 127−132

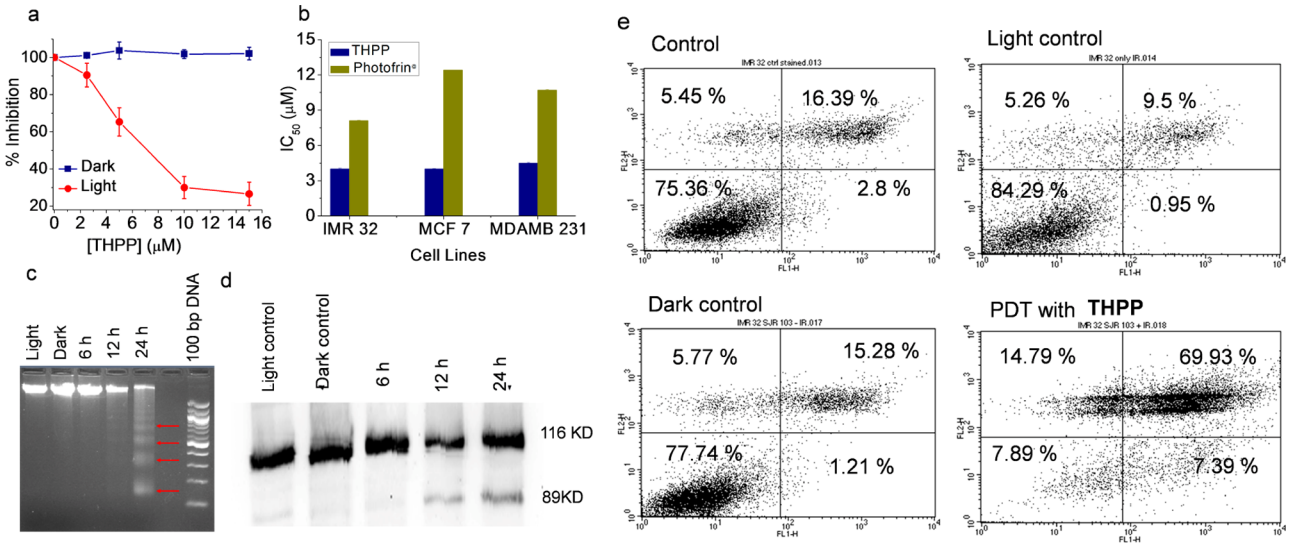

Figure 2. (a) Cytotoxicity of **THPP** in dark (■) and light (●) in IMR 32 cell lines. (b) Comparison of IC_{50} values of **THPP** and Photofrin in IMR 32, MDA MB 231, and MCF 7 cell lines. (c) Fragmentation pattern of genomic DNA after PDT with **THPP** (λ_{irr} > 600 nm). (d) Western blot showing poly(ADP-ribose)polymerase cleavage in SCC 131 cells treated with **THPP**. (e) Flow cytometric analysis of IMR 32 cells after PDT with **THPP**. The lower left quadrant of each panel shows viable cells, negative for Annexin V-FITC/PI, whereas upper right quadrants represent the apoptotic cells, positive for Annexin V-FITC/PI.

cell lines; IMR 32 (human neuroblastoma), MCF 7 (human breast cancer), and MDA MB 231 (aggressive human breast cancer). The light source used was from a commercially available equipment, Waldman PDT 1200L (600−720 nm, 200J cm^{-2}, and 50 mW cm^{-2}).[28] The IC_{50} value, which is a measure of cytotoxic activity, was calculated for all three cell lines (Figure 2). The PDT activity of **THPP** and **Zn-THPP** was compared with the commercial drug, Photofrin, under identical conditions to estimate the efficacy. The percentage cell viability of IMR 32 cells in the presence of **THPP** under different conditions is shown in Figure 2a. **THPP**, interestingly, showed high photocytotoxicity and exhibited IC_{50} values of 4, 4, and 4.5 μM, respectively, in IMR 32, MCF 7, and MDA MB 231 cell lines. As expected, we observed negligible cytotoxicity when these cell lines were treated with **THPP** in the dark (Supplementary Figures 5 and 6). In contrast, Photofrin exhibited relatively higher IC_{50} values of 8.12, 12.4, and 10.7 μM, respectively, for these three cell lines (Figure 2b). The complex **Zn-THPP**, which generated singlet oxygen in near quantitative yields ($\Phi(^1O_2) = 0.92 \pm 0.02$), showed much less photocytotoxicity (IC_{50} value of 18 μM) in MDA MB 231 cells. This observation clearly indicates that the photodynamic activity of a sensitizer in cells not only depends on singlet oxygen yields but also on other parameters such as cellular uptake and retention. The comparison of IC_{50} values indicates that **THPP** exhibits high *in vitro* PDT activity of *ca.* 2−3-fold higher than that of Photofrin in all the tested cell lines.

To understand the mechanism of biological activity, we analyzed the genomic DNA fragmentation through DNA ladder assay, poly(ADP-ribose)polymerase (PARP) cleavage,[29] and comet assay.[30−32] Upon treatment with **THPP** followed by irradiation, we observed DNA ladder in oral cancer cells (SCC 131) (Figure 2c), which was prominent after 24 h. However, no such DNA ladder was observed when the cells were either treated with **THPP** in dark or irradiated without **THPP**. Further, we observed the cleavage of PARP in the presence of **THPP** and light, where the full-length 116 kDa peptide cleaved into 89 kDa (Figure 2d). These results confirm that **THPP** induces time-dependent apoptosis and that a majority of cells showed apoptotic cell death after 24 h. Further evidence was obtained through phase contrast microscopic morphological analysis of cells with and without irradiation (Supplementary Figure 7). We observed significant changes in the morphology from well attached and spread polygonal shaped cells to round and loosely attached ones when the cells were subjected to **THPP** plus light, confirming the apoptotic mediated cell death.

We employed DNA comet assay under neutral (non-denaturing) conditions to understand DNA damage and thereby to provide evidence for apoptotic mechanism. MDA MB 231 cells were treated with **THPP** and were incubated for 1 h. After 3 h post with and without PDT, the cells were subjected to agarose gel electrophoresis. Then, cells were stained with ethidium bromide and analyzed under fluorescence microscope. The fragmented nuclear DNA migrated in an electric field creating a comet-like appearance. The length of the tail is an indication of the extent of DNA damage. We observed the formation of DNA comets only when the cells were given **THPP** plus light. No such comets were observed with **THPP** in the dark, indicating thereby that **THPP** induces DNA fragmentation only upon irradiation (Supplementary Figure 8). In contrast, the usual photosensitizers like Photofrin act mostly on membranes through type II mechanism, whereas in DNA, singlet oxygen mainly induces oxidized guanine.[33]

To further investigate the mechanism of cellular damage, we carried out internucleosomal DNA fragmentation studies through flow cytometric analysis.[34,35] After 12 h of PDT treatment of IMR 32 cells with **THPP**, we observed 7.19% sub-G1 population, which interestingly increased to 39.83% after 24 h. This value is higher than that of 22.26% sub-G1 population observed in the case of Photofrin under similar conditions. These results confirm the enhanced apoptotic potential of **THPP** over Photofrin (Supplementary Figures 9 and 10). In the case of the apoptotic cells, the membrane phospholipid phosphatidylserine is known to be translocated from the inner to outer surface of the plasma membrane, thus exposing it to the external cellular environment. We employed Annexin V-

dx.doi.org/10.1021/cb3004622 | *ACS Chem. Biol.* 2013, 8, 127−132

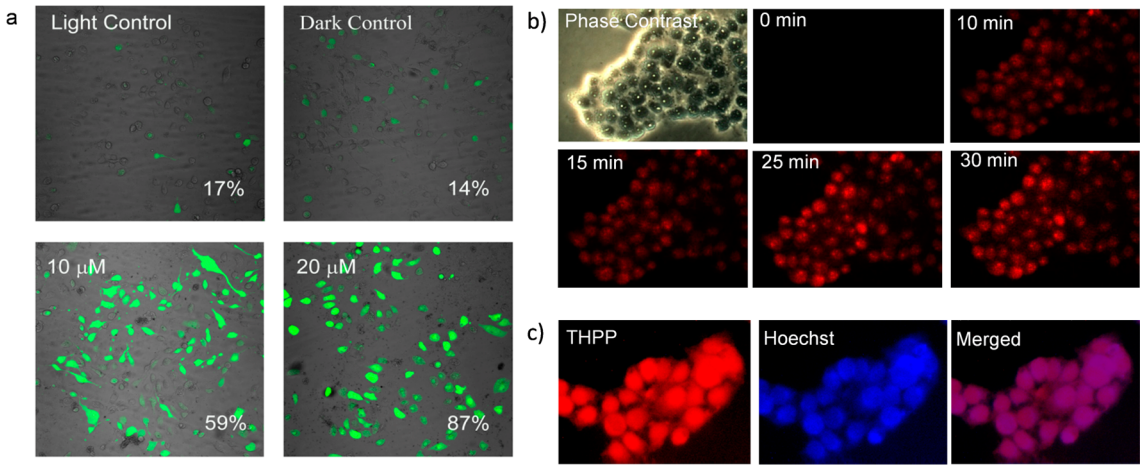

Figure 3. (a) Confocal microscopy images showing concentration-dependent green fluorescence in MDA MB 231 cells after PDT with **THPP** and incubation with ROS tracker CM-H_2DCFDA. (b) Time-dependent fluorescence changes showing cellular uptake of **THPP** in MDA MB 231 cells. (c) Fluorescence images showing localization of **THPP** in MDA MB 231 cells and perfect match of images with Hoechst dye.

FITC, which has high affinity for phosphatidylserine to quantify the formation of the apoptotic cells by fluorescence microscopy and flow cytometry. When IMR 32 cells were treated with **THPP** (10 μM) in dark, we observed that most of the cells were negative for Annexin V-FITC, indicating the negligible formation of apoptotic cells. In contrast, the percentage of cells at the early apoptotic stage increased from 15.28% after 12 h to 69.93% after 24 h, when the cells were subjected to **THPP** and irradiation, thereby confirming that the mechanism of cell death is through the apoptotic pathway.[36,37] Similar observations were made in the flow cytometric analysis of cells treated with **THPP** plus light (Figure 2e).

To understand the reactive oxygen species (ROS) involved, we quantified the generation of ROS in cells during the PDT treatment with **THPP** using 5-(and-6)-chloromethyl-2′,7′-dichlorodihydrofluorescein diacetate acetyl ester (CM-H_2DCFDA) assay. In the reduced form, CM-H_2DCFDA is nonfluorescent, but after cellular oxidation followed by esterases mediated hydrolysis of acetate groups, results in a green fluorescent derivative. When MDA MB 231 cells treated with **THPP** (10 μM) and irradiation followed by the addition of CM-H_2DCFDA, we observed fluorescence in 59% of cells, which increased to 87% with 20 μM of **THPP** (Figure 3a). In contrast, light alone and **THPP** in the dark showed background values of 17% and 14%, respectively. These results demonstrate that only **THPP** upon excitation generates concentration-dependent ROS, which can be attributed to the oxidation of CM-H_2DCFDA and apoptosis mediated cellular death.

To investigate cellular uptake and localization of **THPP**, we employed MDA MB 231 cell lines and compared with Photofrin through fluorescence and confocal microscopic techniques. Interestingly, we observed fluorescence of **THPP** within 10 min (Figure 3b), whereas Photofrin showed negligible uptake even after 30 min of incubation (Supplementary Figure 11) under identical conditions. In the case of **THPP**, we observed that it localizes in the nucleus of the cell, showing intense red emission upon NIR excitation. The nuclear localization was confirmed by the counter staining method using the standard Hoechst dye (Figure 3c). The perfect match of the merged images of the MDA MB 231 cells with both **THPP** and Hoechst dye confirms the nuclear localization of **THPP**. The advantages of **THPP** as a live cell nucleus imaging agent are its fast uptake, intense fluorescence, and NIR excitation, when compared to Hoechst dye, which requires UV light excitation.

In conclusion, we have designed a novel porphyrin derivative **THPP** that showed favorable photophysical properties, negligible dark toxicity, and high *in vitro* PDT activity[38] when compared to the clinically used sensitizer, Photofrin. Our investigations indicated that the biological activity of **THPP** involved predominantly ROS as the reactive intermediates and that the mechanism of cell death is due to apoptosis as confirmed through DNA fragmentation, PARP cleavage, comet assay, morphological changes, and flow cytometric analysis. Uniquely, **THPP** showed fast cellular uptake (<10 min) when compared to Photofrin and localized specifically in the nucleus of the cells. The advantages such as synthetic purity, ease of isolation, high water solubility, high triplet and singlet oxygen yields, fast cellular uptake, specific localization in the nucleus, and high *in vitro* photocytotoxicity make the newly synthesized porphyrin **THPP** an alternate sensitizer for PDT and live cell imaging applications.

METHODS

Calculation of Triplet Quantum Yields and Singlet Oxygen Quantum Yields. Quantum yields of triplet (Φ_T) and singlet oxygen generation (Δ^1O_2) of **THPP** and **Zn-THPP** were determined using an earlier described method[25,26] (Supporting Information).

Determination of Cytotoxicity by Measuring Cellular Proliferation. 3-(4,5-Dimethyl-thiazol-2-yl)-2,5-diphenyltetrazolium bromide (MTT) assay was used for determining cellular proliferation. To human cervical oral cancer cells (SCC 131) were added various sensitizers (2−20 μM), incubated for 1 h, and irradiated at 25 °C using Waldmann PDT 1200 L system, fitted with 1200 W lamp (600−720 nm and 50 mW cm^{-2}). After 24 h of incubation, 10 μL of MTT (5 mg mL^{-1} stock) was added. After 4 h, the supernatant was removed, 100 μL of isopropyl alcohol was added, and the plates were covered with aluminum foil and kept on a shaker until formazan crystals were dissolved. The absorbance at 570 nm was measured, and percentage growth inhibition was calculated as % growth inhibition = (control − test)/control) × 100.

DNA Ladder Assay. SCC 131 cells with and without **THPP** and irradiation were harvested, washed with PBS, and incubated with lysis buffer at 37 °C for 2−3 h. DNA was extracted with isopropanol from the lysate. The precipitated DNA after centrifugation was air-dried and resuspended in tris-HCl overnight at 55 °C. One microgram of DNA was resolved through agarose gel electrophoresis. After staining with

dx.doi.org/10.1021/cb3004622 | *ACS Chem. Biol.* 2013, 8, 127−132

ethidium bromide, the bands were visualized under the Gel Documentation System.

CM-H_2DCFDA Assay. MDA MB 231 cells were treated with sensitizers, incubated for 1 h, and irradiated for 30 min. Immediately after PDT, the cellular reactive oxygen content was determined using CM-H_2DCFDA probe according to the manufacturer's instructions (Invitrogen). The confocal images and differential interference contrast (DIC) images were acquired, merged, and processed using Nikon Imaging Software.

Cellular Uptake and Localization. MDA MB 231 cells were added with various sensitizers and incubated for different periods of time. The images were taken by using phase contrast and fluorescence microscopy. For confirming the nucleus localization, counter staining by standard Hoechst dye was used, and images were taken using appropriate filters.

■ ASSOCIATED CONTENT

Supporting Information

Experimental details including synthesis and supplementary Figures 1−11 showing photophysical and photobiological properties. This material is available free of charge via the Internet at http://pubs.acs.org.

■ AUTHOR INFORMATION

Corresponding Author

*E-mail: rama@niist.res.in or d.ramaiah@gmail.com (D.R.); mrpillai@rgcb.res.in (R.P.); mohan@ccmb.res.in (C.M.R.); tkc@niser.ac.in (T.K.C.).

Notes

The authors declare no competing financial interest.

■ ACKNOWLEDGMENTS

Financial support from DST, CSIR-NIIST, RGCB, CSIR-CCMB, and NISER is gratefully acknowledged. We thank K. G. Anurup and V. G. Parvathy for confocal microscopy analysis. This is contribution no. PPG-333 from CSIR-NIIST, Trivandrum.

■ REFERENCES

(1) Bonnett, R. (2000) Photodynamic action, *Chemical Aspects of Photodynamic Therapy*, Vol. *1*, pp 57−88, Gordon & Breach, London, U.K.

(2) Dolmans, D. E., Fukumura, D., and Jain, R. K. (2003) Photodynamic therapy for cancer. *Nat. Rev. Cancer 3*, 380−387.

(3) Sanchez, M. I., Costas, J. M., Gonzalez, F., Bermudez, M. A., Vazquez, M. E., and Mascareñas, J. L. (2012) *In vivo* light-driven DNA binding and cellular uptake of nucleic acid stains. *ACS Chem. Biol. 7*, 1276−1280.

(4) Keppler, A., and Ellenberg, J. (2009) Chromophore-assisted laser inactivation of α- and γ-tubulin SNAP-tag fusion proteins inside living cells. *ACS Chem. Biol. 4*, 127−138.

(5) Celli, J. P., Spring, B. Q., Rizvi, I., Evans, C. L., Samkoe, K. S., Verma, S., Pogue, B. W., and Hasan, T. (2010) Imaging and photodynamic therapy: mechanisms, monitoring, and optimization. *Chem. Rev. 110*, 2795−2838.

(6) Kadish, K. M., Smith, K. M., Guilard, R. (2002) Synthesis of meso substituted porphyrins, *The Porphyrin Handbook*, Vol. *11*, pp 45−118, Academic Press, New York.

(7) MacDonald, I. J., and Dougherty, T. J. (2001) Basic principles of photodynamic therapy. *J. Porphyrins Phthalocyanines 5*, 105−129.

(8) Avirah, R. R., Jayaram, D. T., Adarsh, N., and Ramaiah, D. (2012) Squaraine dyes in PDT: from basic design to *in vivo* demonstration. *Org. Biomol. Chem. 10*, 911−920.

(9) Arun, K. T., Jayaram, D. T., Avirah, R. R., and Ramaiah, D. (2011) β-Cyclodextrin as a photosensitizer carrier: Effect on photophysical properties and chemical reactivity of squaraine dyes. *J. Phys. Chem. B 115*, 7122−7128.

(10) Thomas, A. P., Saneesh Babu, P. S., Nair, S. A., Ramakrishnan, S., Ramaiah, D., Chandrashekar, T. K., Srinivasan, A., and Radhakrishna Pillai, M. (2012) Meso-tetrakis(*p*-sulfonatophenyl)*N*-confused porphyrin tetrasodium salt: A potential sensitizer for photodynamic therapy. *J. Med. Chem. 55*, 5110−5120.

(11) Devi, D. G., Cibin, T. R., Ramaiah, D., and Abraham, A. (2008) Bis(3,5-diiodo-2,4,6-trihydroxyphenyl)squaraine: A novel candidate in photodynamic therapy for skin cancer models *in vivo*. *J. Photochem. Photobiol., B 92*, 153−159.

(12) Lovell, J. F., Liu, T. W., Chen, J., and Zheng, G. (2010) Activatable photosensitizers for imaging and therapy. *Chem. Rev. 110*, 2839−2857.

(13) Arnbjerg, J., Banzo, A. J., Paterson, M. J., Nonell, S., Borrell, J. I., Christiansen, O., and Ogilby, P. R. (2007) Two-photon absorption in tetraphenylporphycenes: Are porphycenes better candidates than porphyrins for providing optimal optical properties for two-photon photodynamic therapy? *J. Am. Chem. Soc. 129*, 5188−5199.

(14) Bonnett, R., White, R. D., Winfield, U. J., and Berenbaum, M. C. (1989) Hydroporphyrins of the meso-tetra(hydroxyphenyl)porphyrin series as tumour photosensitizers. *Biochem. J. 261*, 277−280.

(15) Detty, M. R., Gibson, S. L., and Wagner, S. J. (2004) Current clinical and preclinical photosensitizers for use in photodynamic therapy. *J. Med. Chem. 47*, 3897−3915.

(16) Schweitzer, V. G. (2001) Photofrin-mediated photodynamic therapy for treatment of early stage oral cavity and laryngeal malignancies. *Lasers Surg. Med. 29*, 305−313.

(17) Jiang, F., Robin, A. M., Katakowski, M., Tong, L., Espiritu, M., Singh, G., and Chopp, M. (2003) Photodynamic therapy with photofrin in combination with buthionine sulfoximine (BSO) of human glioma in the nude rat. *Lasers Med. Sci. 18*, 128−133.

(18) Basu, U., Khan, I., Hussain, A., Kondaiah, P., and Chakravarty, A. R. (2012) Photodynamic effect in near-IR light by a photocytotoxic iron(III) cellular imaging agent. *Angew. Chem., Int. Ed. 51*, 2658−2661; (2012) Photodynamic effect in near-IR light by a photocytotoxic iron(III) cellular imaging agent. *Angew. Chem. 124*, 2712−2715.

(19) Wainwright, M. (2008) Photodynamic therapy: The development of new photosensitisers. *Anti-Cancer Agents Med. Chem. 8*, 280−291.

(20) Ethirajan, M., Chen, Y., Joshi, P., and Pandey, R. K. (2011) The role of porphyrin chemistry in tumor imaging and photodynamic therapy. *Chem. Soc. Rev. 40*, 340−362.

(21) Jisha, V. S., Arun, K. T., Hariharan, M., and Ramaiah, D. (2006) Site-selective binding and dual mode recognition of serum albumin by a squaraine dye. *J. Am. Chem. Soc. 128*, 6024−6025.

(22) Littler, B. J., Miller, M. A., Hung, C.-H., Wagner, R. W., O'Shea, D. F., Boyle, P. D., and Lindsey, J. S. (1999) Refined synthesis of 5-substituted dipyrromethanes. *J. Org. Chem. 64*, 1391−1396.

(23) Littler, B. J., Ciringh, Y., and Lindsey, J. S. (1999) Investigation of conditions giving minimal scrambling in the synthesis of *trans*-porphyrins from dipyrromethanes and aldehydes. *J. Org. Chem. 64*, 2864−2872.

(24) Adarsh, N., Avirah, R. R., and Ramaiah, D. (2010) Tuning photosensitized singlet oxygen generation efficiency of novel aza-BODIPY dyes. *Org. Lett. 12*, 5720−5723.

(25) Ramaiah, D., Joy, A., Chandrasekhar, N., Eldho, N. V., Das, S., and George, M. V. (1997) Halogenated squaraine dyes as potential photochemotherapeutic agents. Synthesis and study of photophysical properties and quantum efficiencies of singlet oxygen generation. *Photochem. Photobiol. 65*, 783−790.

(26) Mathai, S., Smith, T. A., and Ghiggino, K. P. (2007) Singlet oxygen quantum yields of potential porphyrin-based photosensitizers for photodynamic therapy. *Photochem. Photobiol. Sci. 6*, 995−1002.

(27) Redmond, R. W., and Gamlin, J. N. (1999) A compilation of singlet oxygen yields from biologically relevant molecules. *Photochem. Photobiol. 70*, 391−475.

(28) Crosbie, J., Winser, K., and Collins, P. (2002) Mapping the light field of the Waldmann PDT 1200 lamp: potential for wide-field low

light irradiance aminolevulinic acid photodynamic therapy. *Photochem. Photobiol. 76*, 204−207.
(29) Finch, K. E., Knezevic, C. E., Nottbohm, A. C., Partlow, K. C., and Hergenrother, P. J. (2012) Selective small molecule inhibition of poly(ADP-ribose)glycohydrolase (PARG). *ACS Chem. Biol. 7*, 563−570.
(30) Reidy, K., Campanile, C., Muff, R., Born, W., and Fuchs, B. (2012) *m*THPC-mediated photodynamic therapy is effective in the metastatic human 143B osteosarcoma cells. *Photochem. Photobiol. 88*, 721−727.
(31) Shelton, A. H., Rodger, A., and McMillin, D. R. (2007) DNA binding studies of a new dicationic porphyrin. Insights into inter-ligand interactions. *Biochemistry 46*, 9143−9154.
(32) Yuan, Y., Wang, Q., Paulk, J., Kubicek, S., Kemp, M. M., Adams, D. J., Shamji, A. F., Wagner, B. K., Stuart, L., and Schreiber, S. L. (2012) A small-molecule probe of the histone methyltransferase G9a induces cellular senescence in pancreatic adenocarcinoma. *ACS Chem. Biol 7*, 1152−1157.
(33) Ravanat, J.-L., Mascio, P. D., Martinez, G. R., Medeiros, M. H. G., and Cadet, J. (2000) Singlet oxygen induces oxidation of cellular DNA. *J. Biol. Chem. 275*, 40601−40604.
(34) Yslas, E. I., Durantini, E. N., and Rivarola, V. A. (2007) Zinc-(II)-2,9,16,23-tetrakis-(methoxy)phthalocyanine: Potential photosensitizer for use in photodynamic therapy *in vitro*. *Bioorg. Med. Chem. 15*, 4651−4660.
(35) Agarwal, M. L., Clay, M. E., Harvey, E. J., Evans, H. H., Antunez, A. R., and Oleinick, N. L. (1991) Photodynamic therapy induces rapid cell death by apoptosis in L5178Y mouse lymphoma cells. *Cancer Res. 51*, 5993−5996.
(36) Peng, K., Wang, H., Qin, Z., Wijewickrama, G. T., Lu, M., Wang, Z., Bolton, J. L., and Thatcher, G. R. J. (2009) Selective estrogen receptor modulator delivery of quinone warheads to DNA triggering apoptosis in breast cancer cells. *ACS Chem. Biol. 4*, 1039−1049.
(37) Zobel, K., Wang, L., Varfolomeev, E., Franklin, M. C., Elliott, L. O., Wallweber, H. J. A., Okawa, D. C., Flygare, J. A., Vucic, D., Fairbrother, W. J., and Deshayes, K. (2006) Design, synthesis, and biological activity of a potent smac mimetic that sensitizes cancer cells to apoptosis by antagonizing IAPs. *ACS Chem. Biol. 1*, 525−533.
(38) Ramaiah, D., Karunakaran, S. C., Jisha, V. S., Chandrashekar, T. K., Srinivasan, A., Pillai, M. R., Nair, S. A., Saneesh Babu, P. S., Rao, Ch. M., Rao, K. S. (2011) A process for the preparation of novel porphyrin derivatives and their use as PDT agents and fluorescence probes, Patent Appl. WO2011089509A1.